Electronic supporting information for:

Correlation between Cu ion migration behaviour and deNO$_x$ activity in Cu-SSZ-13 for the standard NH$_3$-SCR reaction

Andrew M. Beale*[a,b], Ines Lezcano-Gonzalez[a,b], Wojciech. A. Slawinski[c] and David S. Wragg[c]

[a]Department of Chemistry, University College London, 20 Gordon Street, WC1H 0AJ, London, UK

[b]Research Complex at Harwell, Rutherford Appleton Laboratory, Harwell Science and Innovation Campus, Harwell, Didcot, OX11 0FA, UK

[c]INGAP Centre for Research Based Innovation, Department of Chemistry, University of Oslo, N-0315 Oslo, Norway

*E-mail to: andrew.beale@ucl.ac.uk

1. Experimental details

1.1 Catalyst preparation and characterisation

SSZ-13 zeolite (Si/Al=15) was synthesized as described previously, using *N,N,N*-trimethyladamantammonium in hydroxide form as the structure directing agent in the presence of fluoride, but under static conditions.[1] To obtain the H-form of the zeolite, the as-prepared sample was calcined in air with the following temperature program: 1 °C min^{-1} to 120 °C, held for 2.5 h; 2.2 °C min^{-1} to 350 °C, and 3 h at this temperature; and finally 0.8 °C min^{-1} to 580 °C, and held for 3 h. Cu-SSZ-13-1 (2 wt % Cu; Si/Al=15) was prepared via wet ion exchange (WIE) of the calcined parent zeolite, using an aqueous solution of copper sulphate. Typically, 50 ml of a 0.1 M solution of CuSO$_4$ (Merck, 99 %) was mixed with 1 g of the zeolite and magnetically stirred for 2 h at 80 °C. The product was then recovered by vacuum filtration, washed with deionised water, and dried at 120 °C overnight. The resulting sample was calcined in air with the following temperature program: 2 °C min^{-1} to 120 °C, held for 30 min; and finally 1 °C min^{-1} to 550 °C, and 4 h at this temperature. Cu-SSZ-13-2 (2.5 wt % Cu; Si/Al=22) was prepared via three successive ion exchanges of the parent Cu-SSZ-13-1, following the procedure reported above.

The chemical analysis of the zeolite samples was performed by coupled plasma optical emission spectrometry (ICP-OES, Perkin-Elmer 3300DV instrument). The chemical composition of the zeolite materials – previously reported in reference [2], is shown in Table S1.

Table S1. Chemical composition of the zeolite materials.[2]

Sample	Si/Al	Cu loading (wt %)	I. E. (%)*
Cu-SSZ-13-1	15	2.0	67
Cu-SSZ-13-2	22	2.5	100

* Ion Exchange Level (I.E.); normalized to 100% for a Cu to Al ratio of 1:2.

UV-Vis-NIR DRS data –previously reported in reference [2], was collected using a Varian Cary 500 UV-Vis-NIR spectrometer equipped with a DRS accessory to allow collection in the diffuse reflectance mode. Spectra were collected between 5000-50000 cm^{-1} with a data interval of 10 cm^{-1} and at a rate of 6000 cm^{-1}/min. The UV-Vis spectrum acquired for Cu-SSZ-13-1 zeolite, depicted in Figure S1, shows the presence of isolated Cu^{2+} ions (i.e. 12000 d–d and 47500 cm^{-1} charge transfer (CT) O $\rightarrow$ Cu),[3] while for Cu-SSZ-13-2 zeolite a new band is seen at 40000 cm^{-1}, resulting from the presence of isolated CuO particles.[4]

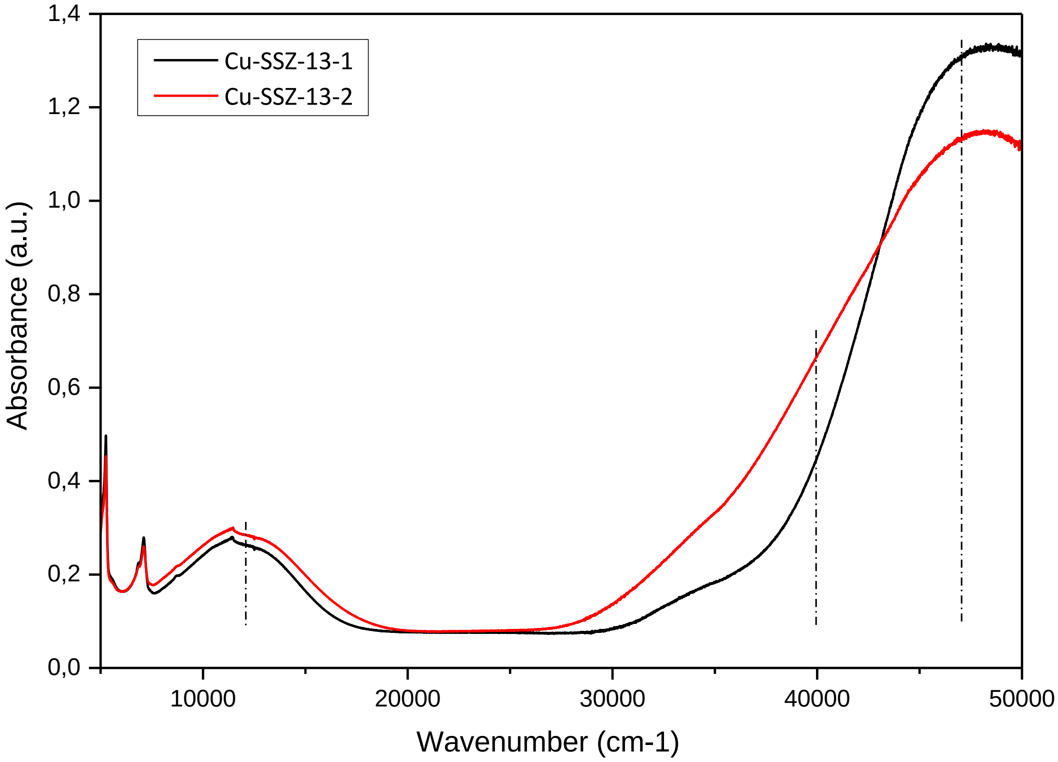

Figure S1. UV-Vis spectra of Cu-SSZ-13-1 and Cu-SSZ-13-2 zeolites.[2]

Further characterisation of the parent and Cu-exchanged SSZ-13 zeolites (i.e. EXAFS, XRD, ^{27}Al NMR, N_2 adsorption, NH_3-TPD, SEM and FT-IR) is reported in a previous study and not repeated herein.[2]

1.2 Comparison in deNO$_x$ activity during standard NH$_3$-SCR of Cu-SSZ-13-1 and Cu-SSZ-13-2 samples

Catalytic tests were performed in a fixed bed plug flow set up. Typically, 150 mg of powdered catalyst material (sieve fractions of 0.425-0.150 mm) were loaded in a 1 cm OD quartz tubular reactor. Prior to the experiment, the zeolite sample was pre-treated for 1 h with 20 % O_2 in He at 550 °C. After the pre-treatment, the desired reaction temperature was fixed and then, the catalyst exposed to a SCR feed composition of 1000 ppm NO, 1000 ppm NH_3 and 5 % O_2, and He for balance, with Gas Hourly Space Velocity (GHSV) of 100,000 h^{-1}. Steady-state measurements were performed at different temperatures, from 100 to 500 °C, using a stabilization period of 30 min at each temperature and analysing the output gases by mass spectrometry (Hiden Analytical, HPR-20 QIC). All SCR gases were provided by Linde. To avoid condensation in the reaction system, all the gas lines were heated to 150 °C.

1.3 Acquisition and analysis of in situ powder diffraction data

Powder X-ray diffraction (PXRD) measurements were performed on the Swiss-Norwegian beamline (SNBL, BM01A) at the European Synchrotron Radiation Facility (ESRF), Grenoble, France. The diffractometer is based on a Huber goniometer with a Pilatus 2M detector. X-rays with a wavelength of 0.69811 Å were used, selected by 2 Rh coated mirrors and a silicon (111) double crystal monochromator. The beamline setup is described in detail elsewhere.[5] Data were collected at a sample to detector distance of 260 mm (calibrated using NIST SRM660b lanthanum hexaboride) and a 2-θ range of 2 to 48.5 ° was used in the Rietveld analysis. Samples of Cu-SSZ-13 were packed between plugs of quartz wool in 0.5 mm quartz capillaries and mounted in a Norby-type flow cell. Three *in situ* experiments were carried out: (1) activation of Cu-SSZ-13-1 by heating to 773 K at a rate of 5 K min^{-1} under a flow of 50 % oxygen in helium, the sample was then cooled to room temperature under a flow of pure helium; (2) activation of Cu-SSZ-13-2 by heating to 773 K at a rate of 5 K min^{-1} under a flow of 50 % oxygen in helium and (3) Heating the activated sample from room temperature to 773 K at a rate of 5 K min^{-1} under a flow of 50 % oxygen in helium followed by cooling to 473 K and followed by reaction using NO (1880 ppm) and NH_3 (1880 ppm) and 6 % O_2 to simulate an SCR feed. The gases were flowed over the cell at rates which combined to give a flow of around 10 ml min^{-1}. Data were collected throughout the process with a data collection time of 10 s per frame and converted to 1-D powder patters using Fit2D and the SNBL scaling software.

For the activation experiments performed on Cu-SSZ-13-1 and Cu-SSZ-13-2 the room temperature powder pattern from data series were used to locate the Cu atoms in the cages from difference Fourier maps. Initial maps were produced by refining against the high angle data only (these are less affected by the non-framework atoms) then fixing the scale factor and refining the whole pattern to obtain the difference maps. The Cu was clearly localized in the 8*r* vicinity (in agreement with the findings of Andersen et al using maximum entropy methods) and two oxygen positons corresponding to adsorbed water were found in subsequent iterations of the mapping process.[6] The water oxygen sites were used as dummy atoms to account for the electron density in the cages (this approach has been used elsewhere and difference Fourier maps were then used to locate the Cu atoms at 773 K in the dataset.[7] These models were then combined to produce a model for parametric Rietveld refinement of the three temperature series. In this model both possible Cu sites (8*r* and 6*r*) were included in the refinement at all temperatures and their occupancies were refined. Initially both Cu atom occupancies were refined freely, however in later refinements we added the parametric constraint that the sum of the two site occupancies must be equal to the total Cu occupancy, with this total occupancy refined parametrically against all powder patterns in the series.[8] The latter method gives a very precise value for the total Cu in the sample by using all the available powder data but makes the assumption that all Cu is always in either of the two sites. Then trends obtained are very similar for both methods. The zero correction was refined against all powder patterns in parallel for each data series. All framework atom positions were refined without restraints along with isotropic thermal parameters for the silicon and oxygen atoms (one parameter for each type), background, peak broadening, scale factor, lattice parameters, and occupancies for the non-framework atoms (a total of 31 refined parameters on each powder pattern plus two parameters refined against the entire dataset). For the parametric refinement of data series (2) the model we have reported elsewhere for Cu-SSZ-13-NO at room temperature was used as a starting point, with the Cu added at the same position as for the activation model.[9] This gave a total of 32 refined parameters for each individual pattern, plus two refined against the entire dataset.

2. Results

2.1 In situ powder diffraction data recorded during activation in air to 500 °C of Cu-SSZ-13-1

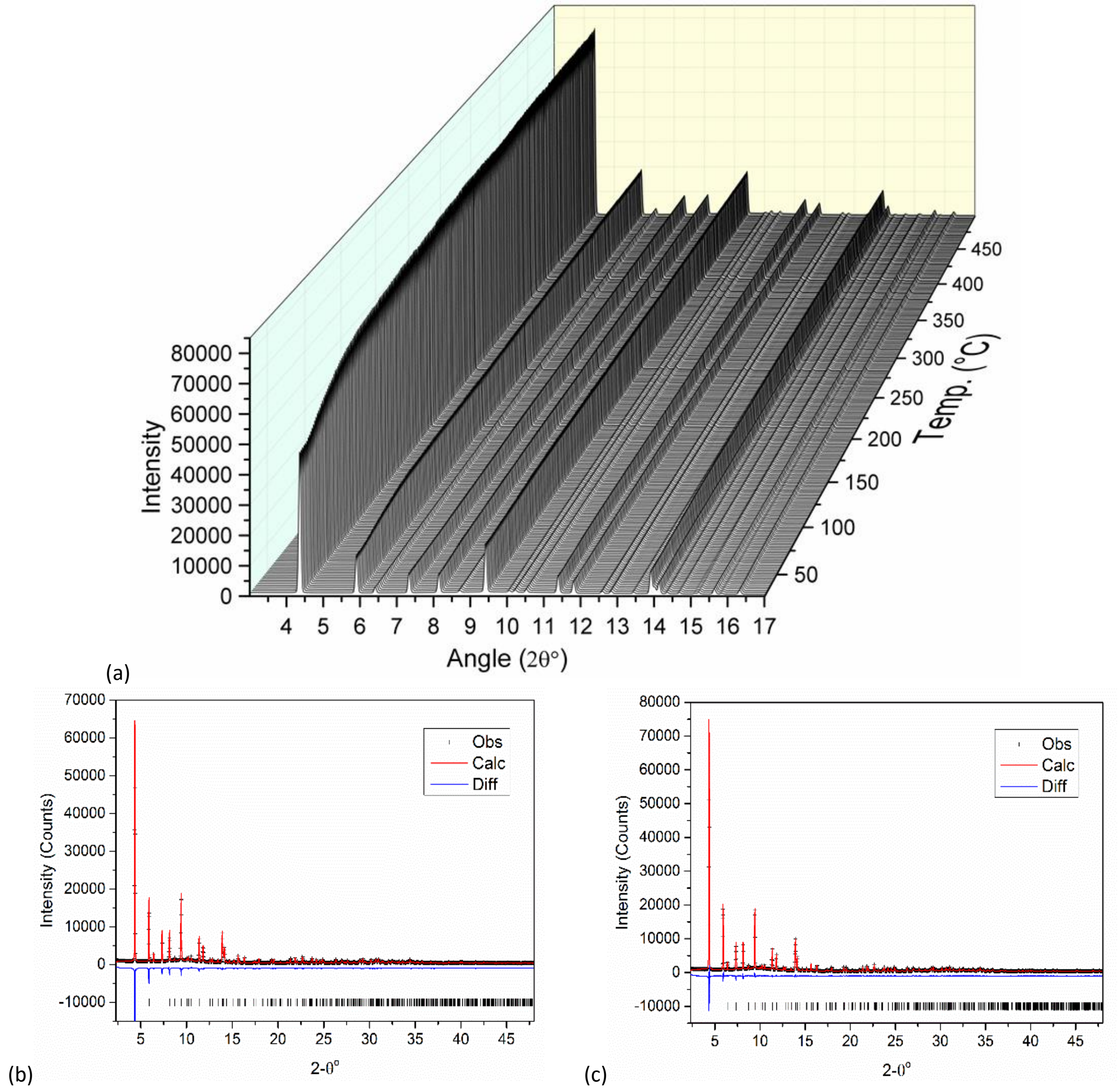

Figure S2. (a) Stack XRD plot and example Rietveld analyses of a single pattern recorded at (b) 100 °C and (c) 500 °C. The data extracted from the Rietveld analysis is listed in Tables S2-4. The accompanying difference Fourier maps from the analyses of the data in (b, c) can be found in Figure 2 in the main text.

Table S2. Rietveld refinement details and results for Cu-SSZ-13-1 at 100 and 500 °C

Radiation, Wavelength (Å)	SNBL beamline BM01A, 0.69811	
Crystal System	Trigonal (hexagonal axes)	
Space Group	R-3m (No.166)	
	Data recorded at 100 °C	**Data recorded at 500 °C**
a, *c* (Å), volume (Å^3)	13.5656(2), 14.7970 (3), 2358.21(8)	13.53697(19), 14.78321(28), 2346.079(80)
Rwp, Rp, Rexp	3.423, 5.222, 0.168	3.502, 4.421, 0.170
Rwp, Rp, Rexp - background	7.798, 7.358, 0.383	9.400, 6.710, 0.456
R Bragg	5.59	1.71
GooF	20.359	20.626
Parameters (powder pattern, all data)	31, 2	31, 2
Restraints	0	0
Constraints	5	5
Number of Data Points (powder pattern)	1554	1554

Table S3. Atomic coordinates, thermal parameters and site occupancies determined from PD data collected on Cu-SSZ-13-1 at 100 and 500 °C

Data recorded at 100 °C					
Atom	**x**	**y**	**z**	**B(eq)(Å^2)**	**Site Occupancy**
Si1	-0.00000(14)	0.228516(99)	0.104026(65)	0.05(2)	1
O1	0.90029(15)	0.09971(15)	0.12260(26)	0.953(45)	1
O2	0.64698(24)	0.64698(24)	0.5	0.953(45)	1
O3	0.12021(16)	0.24043(31)	0.13109(25)	0.953(45)	1
O4	0	0.26466(23)	0	0.953(45)	1
Cu1 (d6*r*)	0	0	0.905(13)	0.2	0.0060(15)
O1W	0.34294	0.67147	0.20358	1.905(90)	0.0161(36)
O2W	0.2663	0.5326	0.2827	1.905(90)	0.0658(69)
Cu2 (8*r*)	0.5	0.5	0	0.2	0.0272(15)
Data recorded at 500 °C					
Si1	0.00044(19)	0.22888(13)	0.103596(83)	0.600(23)	1
O1	0.90094(20)	0.09906(20)	0.12300(35)	2.095(53)	1
O2	0.64587(34)	0.64587(34)	0.5	2.095(53)	1
O3	0.12027(21)	0.24055(42)	0.13157(32)	2.095(53)	1
O4	0	0.26516(31)	0	2.095(53)	1
Cu1 (d6*r*)	0	0	0.9112(32)	0.2	0.0255(18)
O1W	0.34294	0.67147	0.20358	4.19(11)	0.0070(44)
O2W	0.2663	0.5326	0.2827	4.19(11)	0.0516(87)
Cu2 (8*r*)	0.5	0.5	0	0.2	0.0077(18)

Table S4. Bond lengths and angles (selected) determined from PD data collected on Cu-SSZ-13-1 at 100 and 500 °C.

Data recorded at 100 °C			
Atoms	**Bond length (Å)**	**Atoms**	**Bond Angle (°)**
Si1-O1	1.6108(16)	O3-Si1-O4	111.17(19)
Si1-O2	1.6039(19)	O1-Si1-O2	109.32(17)
Si1-O3	1.6070(23)	O2-Si1-O3	108.05(18)
Si1-O4	1.6154(15)	Si1-O3-Si1	149.4(3)
Cu2-O3	3.1854(36)	Si1-O4-Si1	144.63(17)
Cu2-O2W	2.457997(25)		
Data recorded at 500 °C			
Si1-O1	1.618(3)	O3-Si1-O4	111.9(2)
Si1-O2	1.600(4)	O1-Si1-O3	108.3(2)
Si1-O3	1.604(5)	O2-Si1-O3	108.1(2
Si1-O4	1.6094(16)	Si1-O3-Si1	148.4(3)
Cu1-O1	2.376(11)	Si1-O4-Si1	144.2(2)
		Si1-O1-Cu1	100.192(162)

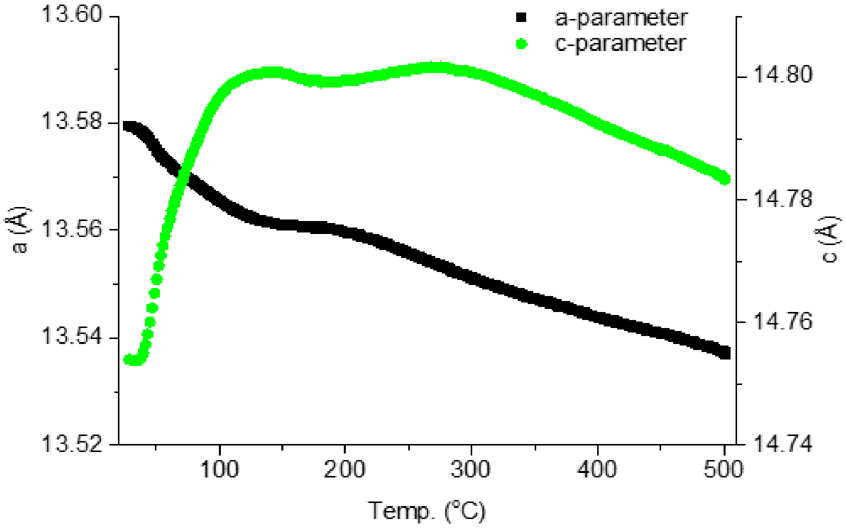

Figure S3. Change in lattice parameters a (green circles) and c (black squares) for Cu-SSZ-13-1 during activation in air to 500 °C. This change in Cu (de)hydration seems to be linked with the expansion in the *c*-parameter whilst the monotonous decay in the *a*-parameter appears to mirror the 8*r* occupancy.

2.2 In situ powder diffraction data recorded during activation of Cu-SSZ-13-2 to 500 °C

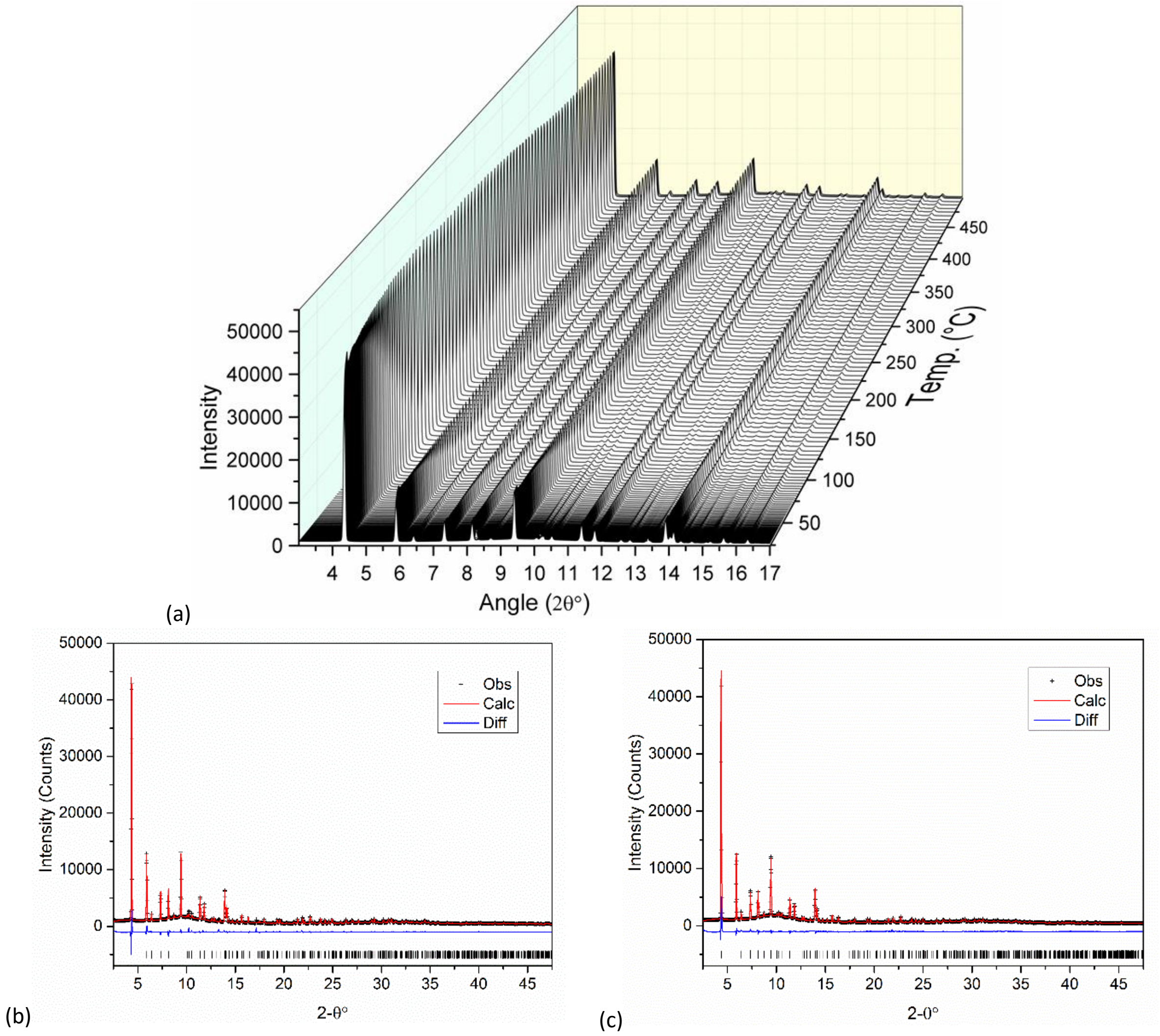

Figure S4. (a) Stack XRD plot and example Rietveld analyses of a single pattern recorded at (b) 100 °C and (c) 500 °C. The data extracted from the Rietveld analysis is listed in Tables S5-7. The accompanying difference Fourier maps from the analyses of the data in (b, c) can be found in Figure S5.

Table S5. Rietveld refinement details and results for Cu-SSZ-13-2 at 100 and 500 °C

Radiation, Wavelength (Å)	SNBL beamline BM01A, 0.69811	
Crystal System	Trigonal (hexagonal axes)	
Space Group	R-3m (No.166)	
	Data recorded at 100 °C	**Data recorded at 500 °C**
a, *c* (Å), volume (Å^3)	13.56166(17), 14.7535(3), 2349.91(9)	3.52577(22), 4.76557(43), 2339.40(10)
Rwp, Rp, Rexp	3.982 , 4.320, 0.181	3.318, 4.018, 0.181
Rwp, Rp, Rexp - background	12.486, 7.689, 0.568	12.246, 7.751,0.669
R Bragg	2.526	3.542
GooF	21.990	18.313
Parameters	29, 4	29, 4
Restraints	0	0
Constraints	5	5
Number of Data Points	1554	1554

Table S6. Atomic coordinates, thermal parameters and site occupancies determined from PD data collected on Cu-SSZ-13-2 at 100 and 500 °C

Data recorded at 100 °C					
Atom	**x**	**y**	**z**	**B(eq)(Å^2)**	**Site Occupancy**
Si1	0.00044(25)	0.22883(17)	0.10429(11)	0.050(30)	1
O1	0.90066(26)	0.09934(26)	0.12380(46)	1.010(68)	1
O2	0.64640(43)	0.64640(43)	0.5	1.010(68)	1
O3	0.12027(27)	0.24053(55)	0.13293(43)	1.010(68)	1
O4	0	0.26366(38)	0	1.010(68)	1
O1w	0.34294	0.67147	0.20358	2.02(14)	0.0274(62)
O2w	0.2663	0.5326	0.2827	2.02(14)	0.037(12)
Cu2 (8*r*)	0.5	0.5	0	0.2	0.0224(24)
Data recorded at 500 °C					
Si1	0.00091(29)	0.22930(20)	0.10345(13)	0.698(37)	1
O1	0.90074(30)	0.09926(30)	0.12314(54)	2.245(85)	1
O2	0.64498(52)	0.64498(52)	0.5	2.245(85)	1
O3	0.12004(32)	0.24009(64)	0.13364(49)	2.245(85)	1
O4	0	0.26411(47)	0	2.245(85)	1
Cu1	0	0	1.0832(72)	0.2	0.0163(27)
O1w	0.34294	0.67147	0.20358	4.49(17)	0.0082(63)
O2w	0.2663	0.5326	0.2827	4.49(17)	0.022(13)
Cu2 (8*r*)	0.5	0.5	0	0.2	0.0060(27)

Table S7. Bond lengths and angles (selected) determined from PD data collected on Cu-SSZ-13-2 at 100 and 500 °C.

Data recorded at 100 °C			
Atoms	**Bond length (Å)**	**Atoms**	**Bond Angle (°)**
Si1-O1	1.619(4)	O3-Si1-O4	111.9(3)
Si1-O2	1.598(5)	O1-Si1-O2	108.9(3)
Si1-O3	1.609(7)	O2-Si1-O3	108.0(3)
Si1-O4	1.611(2)	Si1-O3-Si1	148.0(4)
Cu2-O3	3.151(6)	Si1-O4-Si1	145.6(3)
Cu2-O2W	2.457		
Data recorded at 500 °C			
Si1-O1	1.622(5)	O3-Si1-O4	113.1(4)
Si1-O2	1.596(7)	O1-Si1-O3	107.8(4)
Si1-O3	1.607(7)	O2-Si1-O3	107.9(3)
Si1-O4	1.600(3)	Si1-O3-Si1	146.5(5)
Cu1-O1	2.40(2)	Si1-O4-Si1	145.3(4)
		Si1-O1-Cu1	99.5(6)

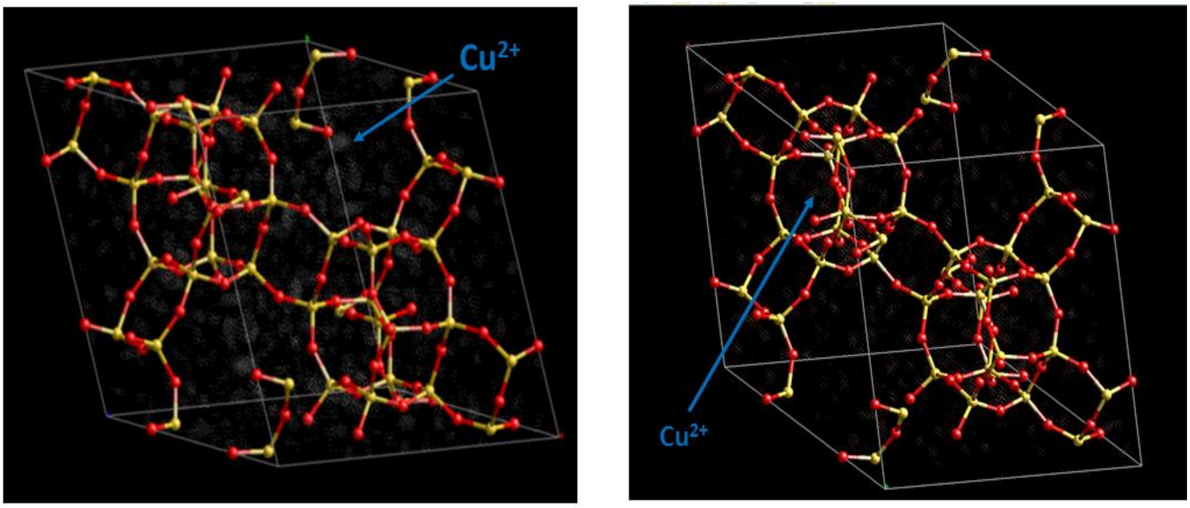

(a) (b)

Figure S5. Difference Fourier map of Cu-SSZ-13-2 sample recorded at 100 °C (a) and 500 °C (b) respectively during activation. Atom colour key (framework): Si^{4+}/Al^{3+} - Yellow, O^{2-} - Red. White clouds represent regions of electron density. In (a) the strongest electron density cloud is clearly located in the vicinity of the 8*r*/*cha* cage which was assigned again to Cu^{2+}. In (b) the map is less clear but again there is no obvious contribution in the 8*r*/*cha* cage that can be assigned to a significant portion of Cu^{2+} whereas a significant sphere of electron density does appear in the 6*r* which we again assign to Cu^{2+}.

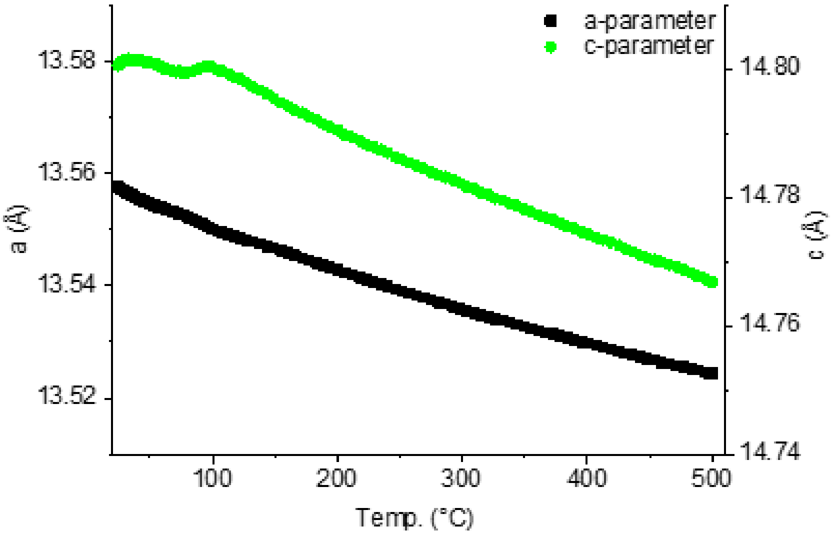

Figure S6. Change in lattice parameters *a* (green circles) and *c* (black squares) for Cu-SSZ-13-2 during activation in air to 500 °C. Changes in the lattice parameters are again quite different to that seen in Cu-SSZ-13-1 with both parameters seen to decrease with increasing temperature (negative thermal expansion).

2.3 XAFS data recorded in situ during activation at 500 °C

Separate in situ XAFS measurements were performed at the Dutch-Belgian beamline (DUBBLE, BM26A) at the European Synchrotron Research Facility (ESRF), Grenoble, France. DUBBLE offers a pre-set gas rig, thereby enabling in situ measurements without the need of assembling additional setups. To adapt to the laboratory plug-flow conditions, sieved fractions of samples were packed into quartz capillaries (1 mm diameter respectively) before the samples (Cu-SSZ-13-1 and Cu-SSZ-13-2 respectively) were calcined to 773 K in a 20 % O_2/He flow (20 ml/min) before in situ transmission XAFS measurements were performed using a Si(111) double crystal monochromator with data recorded at the Cu K-edge (8979 eV). Acquisition was performed over several minutes, to obtain good statistics (signal-to-noise) for the data collected. The X-ray absorption data were background corrected using Athena (IFFEFIT software package).[10] A second-order polynomial was fitted to the raw data in the pre-edge region followed by a cubic spline with k^2-weighting through the post-edge region. The edge jump was defined by extrapolating the spline background to the edge energy (8979 eV) and multiplying the background-subtracted data by a scale factor to give an edge jump of 1.0 (see Figure S7 (a)). The FT of the k^3-weighed data were phase corrected and are plotted in Figure S7 (b, c).

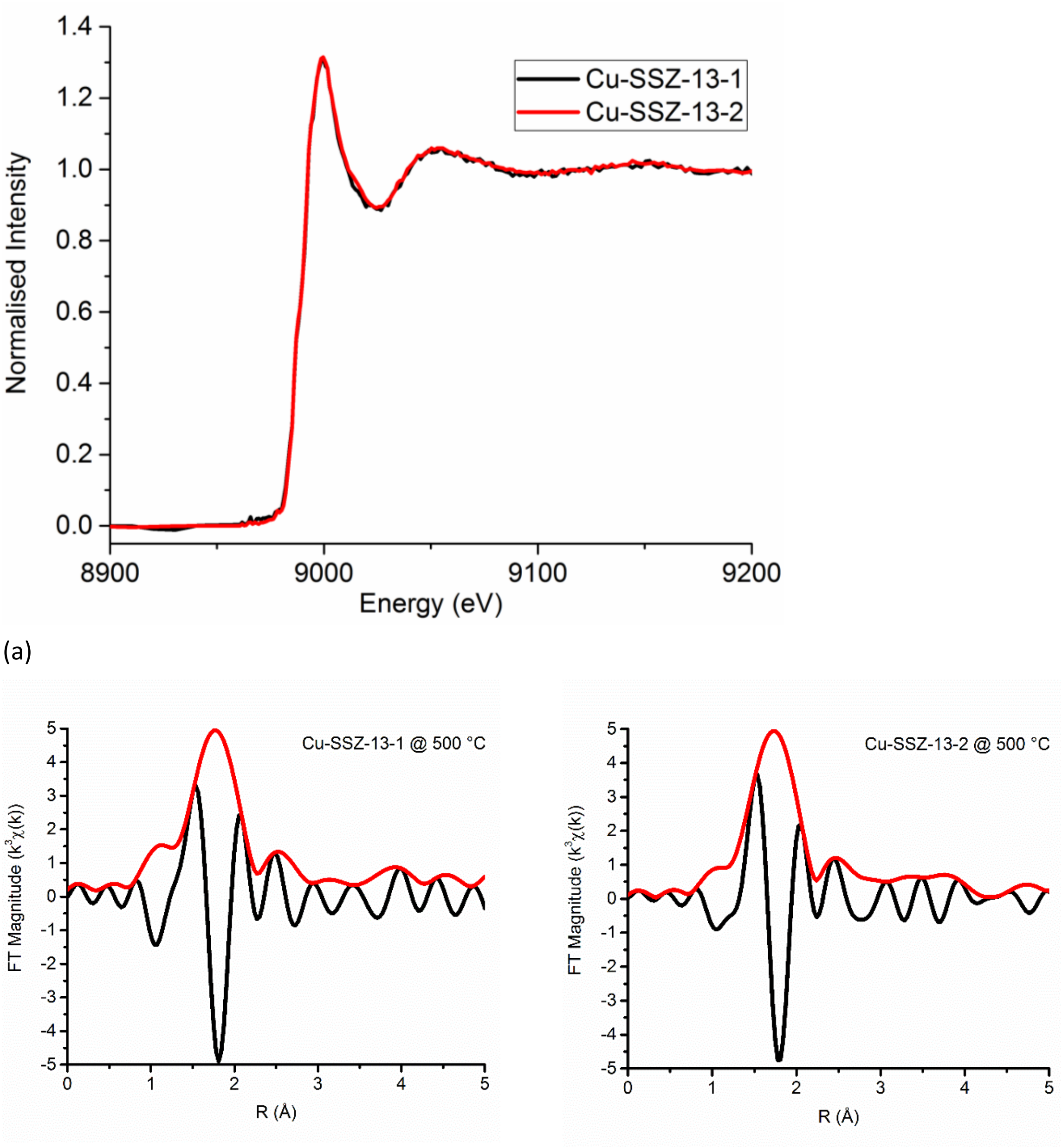

(a)

(b)

(c)

Figure S7. (a) XANES and EXAFS-FT data recorded at the Cu K-edge during activation at 500 °C. Note the strong similarities in the position and intensity of the main peak in the FT which has previously been assigned to 3 Cu-O contributions at a distance of 1.95 Å.

2.4 In situ powder diffraction data recorded on Cu-SSZ-13-1 at 200 °C during the standard NH_3-SCR reaction

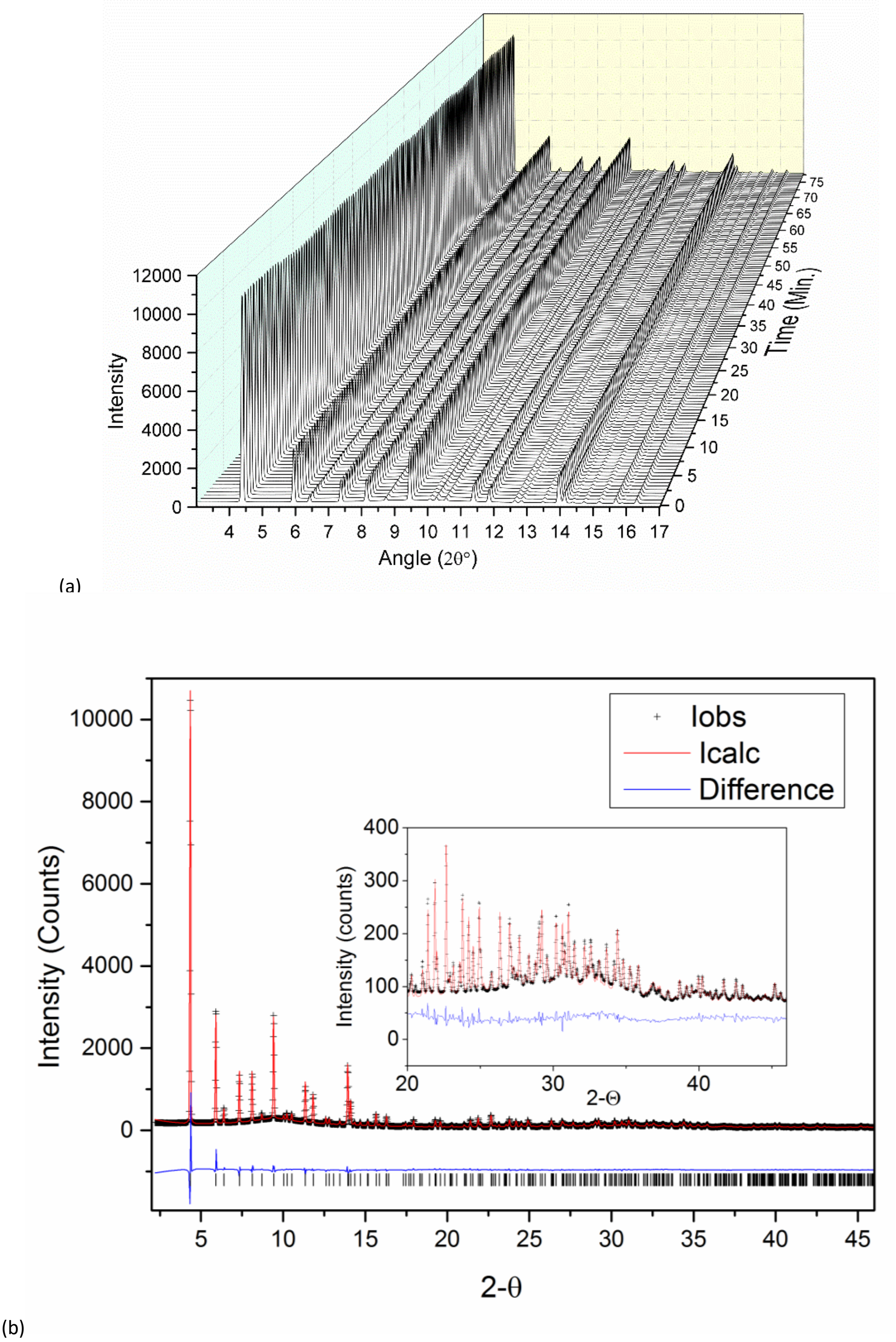

Figure S8. (a) Stack XRD plot and example Rietveld analyses of a single pattern recorded at 200 °C (for ~ 80 min) during the standard NH_3-SCR reaction on sample Cu-SSZ-13-1. The data extracted from the Rietveld analysis is listed in Tables S8-10. The accompanying difference Fourier maps from the analyses of the data in (b, c) can be found in Figure S10.

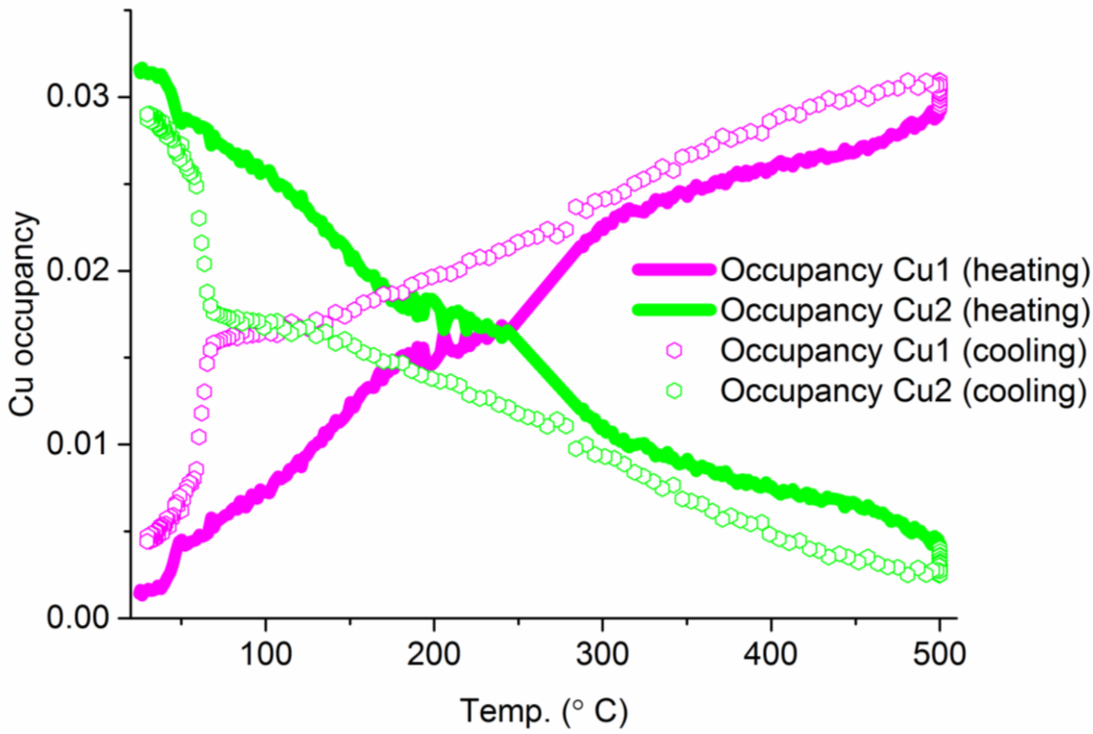

Figure S9. Plots of Cu site occupancy in the 8*r* (solid green line and green hexagons) and 6*r* (solid magenta line and magenta hexagons) as a function of a temperature ramp in a gas stream of 5 % O_2 in He up to 500 °C (solid lines) and cooling to room temperature (hexagons) in Cu-SSZ-13-1. Note the hysteresis in the plot can be explained by the presence of adsorbates on the Cu ions on heating that are not present in the gas stream on cooling.

Table S8. Rietveld refinement details and results Cu-SSZ-13-1 during the standard SCR reaction at 200°C

Radiation, Wavelength (Å)	SNBL beamline BM01A, 0.69811
Crystal System	Trigonal (hexagonal axes)
Space Group	R-3m (No.166)
	Data recorded at 200 °C
a, *c* (Å), volume (Å^3)	13.56166(17), 14.7535(3), 2349.91(9)
Rwp, Rp, Rexp	3.982 , 4.320, 0.181
Rwp, Rp, Rexp - background	12.486, 7.689, 0.568
R Bragg	2.526
GooF	21.990
Parameters	29, 4
Restraints	0
Constraints	5
Number of Data Points	1554

Table S9. Atomic coordinates, thermal parameters and site occupancies determined from PD data collected on Cu-SSZ-13-1 during the standard SCR reaction at 200 °C

Data recorded at 200 °C					
Atom	**x**	**y**	**z**	**B(eq)(Å^2)**	**Site Occupancy**
Si1	0.00044(25)	0.22883(17)	0.10429(11)	0.050(30)	1
O1	0.90066(26)	0.09934(26)	0.12380(46)	1.010(68)	1
O2	0.64640(43)	0.64640(43)	0.5	1.010(68)	1
O3	0.12027(27)	0.24053(55)	0.13293(43)	1.010(68)	1
O4	0	0.26366(38)	0	1.010(68)	1
O1w	0.34294	0.67147	0.20358	2.02(14)	0.0274(62)
O2w	0.2663	0.5326	0.2827	2.02(14)	0.037(12)
Cu2 (8R)	0.5	0.5	0	0.2	0.0224(24)

Table S10. Bond lengths and angles (selected) determined from PD data collected on Cu-SSZ-13-1 during the standard SCR reaction at 200 °C.

Data recorded at 200 °C			
Atoms	**Bond length (Å)**	**Atoms**	**Bond Angle (°)**
Si1-O1	1.619(4)	O3-Si1-O4	111.9(3)
Si1-O2	1.598(5)	O1-Si1-O2	108.9(3)
Si1-O3	1.609(7)	O2-Si1-O3	108.0(3)
Si1-O4	1.611(2)	Si1-O3-Si1	148.0(4)
Cu2-O3	3.151(6)	Si1-O4-Si1	145.6(3)
Cu2-O2W	2.457		

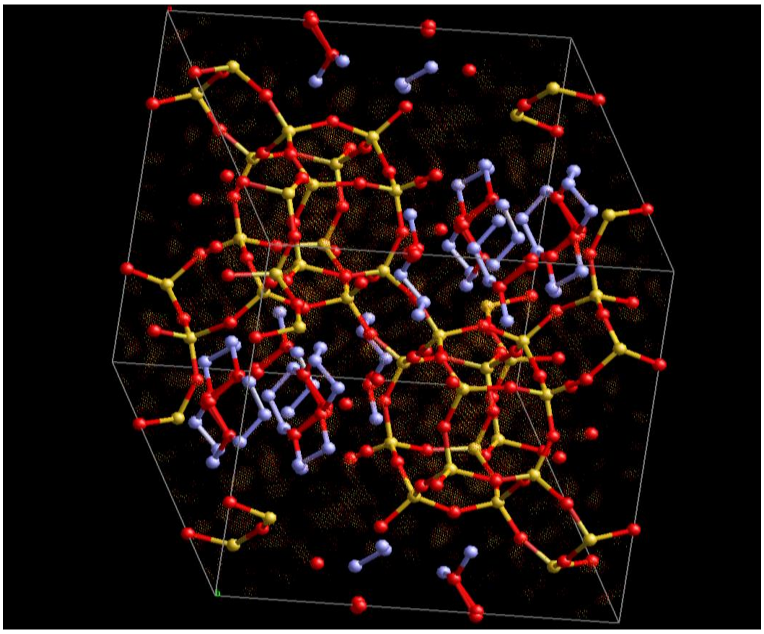

Figure S10. Difference Fourier map of Cu-SSZ-13-1 sample recorded at 200 °C during the standard NH_3-SCR reaction. Atom colour key (framework): Si^{4+}/Al^{3+} - Yellow, O^{2-} - Red, N - light blue. Note NO_x and water atoms were left in the model during the calculation of difference Fourier maps. White clouds represent regions of unassigned electron density. The strongest electron density cloud is clearly located in the vicinity of the 6*r* which was assigned again to Cu^{2+}. Some electron density can be still observed in the 8*r* although the occupancy of this site as determined using Rietveld refinement is ~ 50 % of the occupancy of Cu^{2+} in the 6*r*.

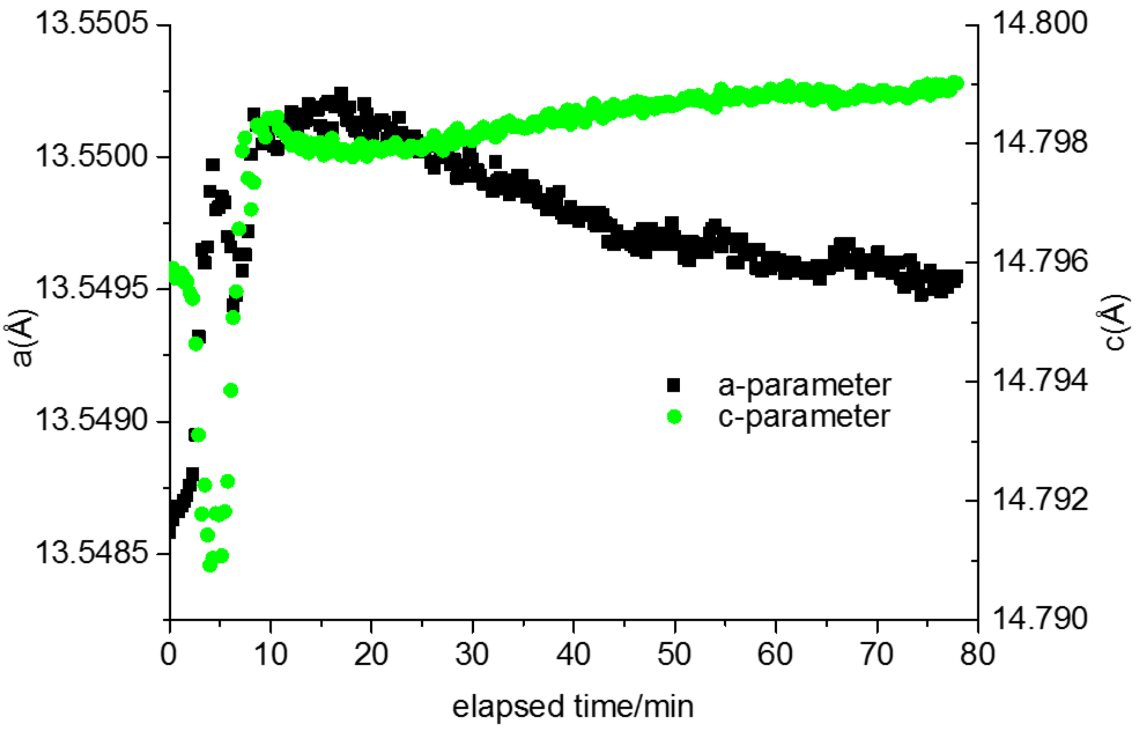

Figure S11. Change in lattice parameters *a* (green circles) and *c* (black squares) for Cu-SSZ-13-1 during the standard NH_3-SCR process at 200 °C. The spike/reversal in the behavior of the c-parameter seen after 5 min. is most likely caused by the filling of the zeolite pores with the SCR gases.

3. Acknowledgements

The authors A. M. Beale and I. Lezcano-Gonzalez acknowledge EPSRC for funding. Dmitri Chernyshov (beamline scientist, SNBL) is thanked for his contribution towards enabling the measurements to be performed.

4. Copies of raw data

Link to copies of experimental data i.e. radially integrated XRD data and results from parametric refinements, XAFS data can be found at http://tiny.cc/C6CC00513F

5. References

[1] M. Moliner, C. Franch, E. Palomares, M. Grill, A. Corma, *Chem. Commun.* **2012**, *48*, 8264-8266.

[2] I. Lezcano-Gonzalez, U. Deka, B. Arstad, A. Van Yperen-De Deyne, K. Hemelsoet, M. Waroquier, V. Van Speybroeck, B. M. Weckhuysen, A. M. Beale, *Phys. Chem. Chem. Phys.* **2014**, *16*, 1639-1650.

[3] M. H. Groothaert, J. A. van Bokhoven, A. A. Battiston, B. M. Weckhuysen, R. A. Schoonheydt, *J. Am. Chem. Soc.* **2003**, *125*, 7629-7640.

[4] A. El-Trass, H. ElShamy, I. El-Mehasseb, M. El-Kemary, *Appl. Surf. Sci.* **2012**, *258*, 2997-3001.

[5] W. van Beek, O. V. Safonova, G. Wiker, H. Emerich, *Phase Transitions* **2011**, *84*, 726-732.

[6] C. W. Andersen, M. Bremholm, P. N. R. Vennestrom, A. B. Blichfeld, L. F. Lundegaard, B. B. Iversen, *IUCrJ* **2014**, *1*, 382-386.

[7] a) D. S. Wragg, F. L. Bleken, M. G. O'Brien, M. Di Michiel, H. Fjellvag, U. Olsbye, *Phys. Chem. Chem. Phys.* **2013**, *15*, 8662-8671; b) D. S. Wragg, M. G. O. Brien, F. L. Bleken, M. Di Michiel, U.

Olsbye, H. Fjellvag, *Angew. Chem.-Int. Edit.* **2012**, *51*, 7956-7959; c) D. S. Wragg, D. Akporiaye, H. Fjellvag, *J. Catal.* **2011**, *279*, 397-402.
[8] G. W. Stinton, J. S. O. Evans, *J. App. Cryst.* **2007**, *40*, 87-95.
[9] I. Lezcano-Gonzalez, D. S. Wragg, W. A. Slawniski, K. Hemelsoet, A. Van Yperen-De Deyne, M. Waroquier, V. Van Speybroeck, A. M. Beale, *J. Phys. Chem. C* **2015**.
[10] a) M. Newville, *J. Synchr. Rad.* **2001**, *8*, 322-324; b) B. Ravel, M. Newville, *J. Synchr. Rad.* **2005**, *12*, 537-541.